BEAM DYNAMICS STUDIES OF THE 8-GeV SUPERCONDUCTING H$^-$ LINAC*

P.N. Ostroumov†, B. Mustapha and V.N. Aseev, ANL, Argonne, IL 60439, USA

Abstract

A pulsed 8-GeV H$^-$ linac has been proposed to enhance the accelerator complex at Fermilab as a high-intensity neutrino source. The linac is based on 430 independently phased superconducting cavities. The front-end of the linac (up to 420 MeV) operating at 325 MHz is based on RIA-type multi-spoke cavities. The rest of the linac (from 420 MeV to 8 GeV) uses ILC-type elliptical cavities. We have performed large scale end-to-end beam dynamics simulations of the driver linac using the code TRACK including all sources of machine errors and detailed beam loss analysis. The results of these simulations are presented and discussed.

INTRODUCTION

A multi-mission 8 GeV injector linac was proposed to replace the existing Fermilab Booster [1]. Among the missions of such linac is to provide more beam power at the end of the linac and the Main Injector (MI), allow more flexibility for the MI energy, possibility of accelerating both e- and protons. The linac will also serve the neutrino factory (NUMI, NUTEV) and a fixed target program and to produce "Super beams" of neutrinos to Homestake.

A multi-megawatt (2-4 MW) superconducting linac has been proposed to serve as the Fermilab Proton Driver (FNAL-PD). The basic parameters of the linac are listed in table 1.

Table 1: Basic Parameters of the Linac

Parameter	Value
Beam particle	H$^-$
Output beam energy	8 GeV
Beam peak current	40 mA
Beam current averaged over the pulse	25 mA
Pulse length	1 msec
Pulse repetition rate	10 Hz
Beam Pulsed power	200 MW
Beam average power	2 MW
Wall power	12.5 MW
Total length	678 m

After briefly reviewing the current lattice design of the FNAL-PD, we present and discuss the results of large scale beam dynamics simulations including all sources of machine error using the code TRACK [2]. A beam loss analysis is also performed in order to study error tolerances.

FNAL-PD LATTICE DESIGN

A schematic layout of the proposed lattice design is shown in figure 1. As indicated, the initial acceleration and focusing will be provided by an RFQ. The MEBT will provide a space for a fast chopper and match the beam to the following linac section. The whole design (RFQ, MEBT and Linac) has been iterated several times to satisfy more advanced RFQ beam specifications [3]. As figure 1 shows, the linac is subdivided into 7 sections where either the type of cavity or the focusing is different, see table 2. The linac is based on 430 independently phased superconducting cavities. The front-end of the linac (up to 420 MeV) operating at 325 MHz is based on RIA-type multi-spoke cavities [4]. The rest of the linac (from 420 MeV to 8 GeV) uses ILC-type elliptical cavities [5]. More details about the design can be found in [6].

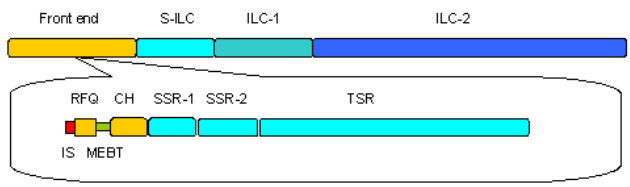

Figure 1: Schematic layout of the FNAL-PD linac.

Table 2: Different linac sections with cavity and focusing types as well as the output energy. For focusing we used S:Solenoid, R:Resonator, nR: n Resonators, F:Focusing quad., and D:Defocusing quad.

#	Section Name	Cavity Type	Focusing Type	W$_{out}$ (MeV/u)
1	CH	X-Bar H-Type	SR	10
2	SSR-1	Single spoke 1	SR	32
3	SSR-2	Single spoke 2	S2R	123
4	TSR	Triple spoke	FRDR	418
5	S-ILC	Elliptic 8 cells	F2RD2R	1213
6	ILC-1	Elliptic 9 cells	F4RD3R	2424
7	ILC-2	Elliptic 9 cells	F8RD8R	7934

* Work supported by the U.S. Department of Energy, Office of Nuclear Physics, under Contract No. W-31-109-ENG-38.

† ostroumov@phy.anl.gov

BEAM DYNAMICS SIMULATIONS

The Code TRACK

The beam dynamics code TRACK has been developed at Argonne over the last few years [7]. TRACK is a ray-tracing code that was originally developed to fulfill the special requirements of the RIA (Rare Isotope Accelerator) accelerator systems [8]. It is, however, a general beam dynamics code for hadron linacs (protons and heavy-ions) design and simulation with possible extension to electron linacs. The most recent version of TRACK supports an extensive number of different types of beam line elements with 3D fields including fringe fields. 3D space charge forces for intense beams are included by solving the Poisson equation of the beam after every tracking step. It also includes the simulation of all possible sources of machine errors, beam monitoring tools, corrective transverse steering and longitudinal corrections as well as automatic longitudinal and transverse tuning of single and multiple charge state beams. Reference [2] contains a brief description of the code. For more details with specific applications of TRACK, see [9] and [10].

Error Simulations

The main sources of error in the FNAL-PD linac are element misalignments and the precision and stability of the RF system. The different errors as well as their typical values are listed in Table 3. In a given simulation, the actual errors are randomly generated according to the corresponding distribution. The uniform distributions are generated between the extreme values $\pm$ max. The Gaussian distributions are truncated at $\pm$ 3 rms value. The displacement errors are applied to the x and y positions of elements ends. The rotation errors are applied around the z axis (beam axis). For statistical significance the simulations were repeated 100 times starting every time from a different seed for the random number generator. 1 million particles were tracked in every simulation. These large scale simulations were performed using the parallel version of TRACK on the Jazz cluster at Argonne [11].

Table 3: Typical Values of Misaligment and RF Errors

Error	Value	Distr.
Cav. end displacement RT and SC spoke cav. SC elliptical cav.	 0.5 mm (max) 1.0 mm (max)	Uniform
Sol. end displacement Type 1 (18 cm long) Type 1 (32 cm long)	 0.15mm (max) 0.2 mm (max)	Uniform
Quad. end displacement	0.15mm (max)	Uniform
Quad. rotation (z-axis)	5 mrad (max)	Uniform
Cav. field jitter error	0.5 % (rms)	Gaussian
Cav. phase jitter error	0.5^o(rms)	Gaussian

In order to study the individual effect of misalignment and RF errors, we performed a first set of simulations without RF errors (0%, 0^o) and a second set with RF errors (1%, 1^o). Each of these cases were simulated using 100 seeds with 1M particles per seed. Figure 2 shows the beam envelopes obtained in both cases. We notice that while the effect of RF errors is limited on transverse beam envelopes, it is rather significant on the phase envelope. In figure 3, the RMS beam emittances are shown. We clearly see that the effect of RF errors on the transverse emittances is significant which is due to a strong coupling between the longitudinal and transverse motion due to relatively weak focusing (long focusing periods in the TSR to S-ILC transition). In conclusion, the RF errors have more impact on the beam dynamics than the misalignment errors.

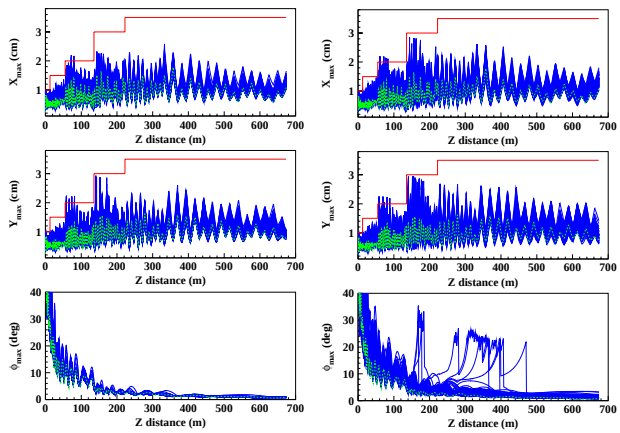

Figure 2: Beam envelopes in X, Y and phase. The left 3 plots are for RF errors of (0%, 0^o) and the right ones are for (1%, 1^o). The plots show in solid-blue the superposition of the results from 100 set of errors (seeds). The dashed-green curves corresponds to the reference case with no errors at all and the horizontal solid-red lines show the beam line aperture.

Beam Loss Analysis

The study of error tolerances through the analysis of beam loss requires the simulation of different combinations of error amplitudes. Since the design is more sensitive to RF errors, we choose to keep the misalignment errors at their typical values of table 3 and vary only the RF errors. It is important to mention that we are including only RF jitter or dynamic errors assuming that RF static errors could be corrected for. It is also important to note that for Gaussian distributions with rms values of (1%, 1^o), the actual errors could reach the extreme values of (3%, 3^o).

In addition to the cases of (0%, 0^o) and (1%, 1^o) presented above we simulated the case of (2%, 2^o). The results in the form of fraction beam loss and the peak beam power lost are given in table 4. We notice that from being negligible for (1%, 1^o) the losses are more significant for (2%, 2^o) exceeding the workable limits in both beam frac-

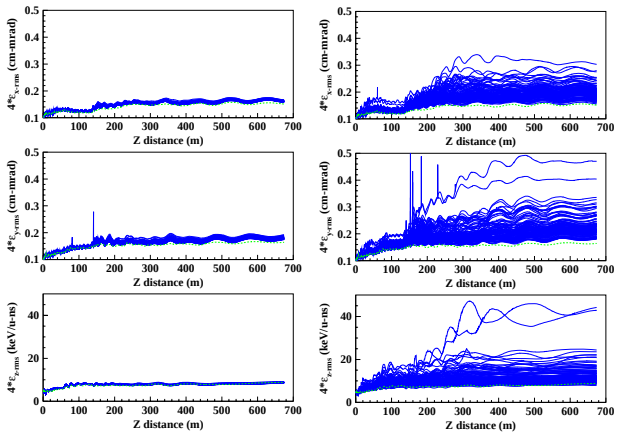

Figure 3: Beam 4×RMS emittances in the 3 phase space planes. The left 3 plots are for RF errors of (0%, 0^o) and the right ones are for (1%, 1^o). The line and color index is the same as figure 2.

tion and peak loss. Figure 4 shows the beam power loss in Watts/m along the linac indicating the exact locations of the beam loss.

The case of (2%, 2^o) corresponds to extreme values of (6%, 6^o) which are very large explaining the significant beam loss observed. In most cases RF jitter errors could be controlled to be below (0.5%, 0.5^o) using fast feed-back systems. Errors with variation time larger than 100 μs could usually be eliminated using such systems leaving a less important faster component of about (0.5%, 0.5^o). So the case of (2%, 2^o) is an extreme case that we simulated only to show the tolerance limits of the actual design. The major fraction of beam loss takes place at the beginning of the S-ILC section where the frequency jumps by a factor of 4 from 325 MHz to 1300 MHz. To avoid such losses the slow component of energy-phase errors (~ 100 μs) must be corrected by including several resonators from the preceding TSR section into a beam based feed-back system for the S-ILC section.

Table 4: Beam fraction lost and peak power loss for different values of RF errors. The misalignment errors are kept unchanged at their values of table 3.

RF Errors	Beam fraction lost	Peak power loss
0 %, 0^o	2×10^{-5}	0.1 Watts/m
1 %, 1^o	1×10^{-4}	0.4 Watts/m
2 %, 2^o	3×10^{-2}	35 Watts/m

SUMMARY

We have performed large scale beam dynamics simulations of the FNAL-PD driver linac including all sources of machine error. The effect of both misalignment and RF errors were studied showing more sensitivity to RF errors. A

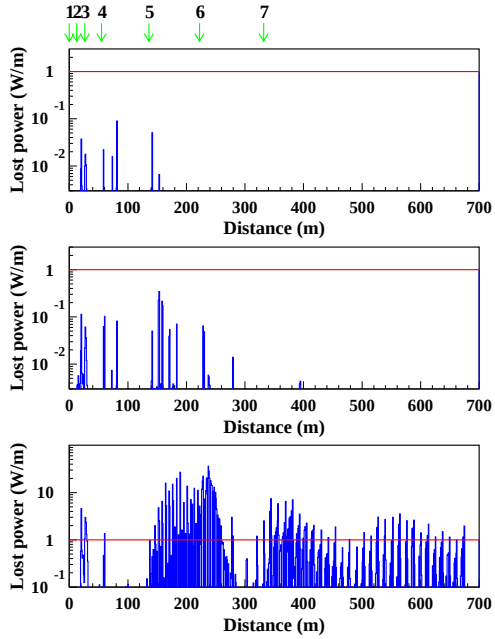

Figure 4: Beam loss in Watts/m along the FNAL-PD linac for different RF errors: (0%, 0^o) for the top plot, (1%, 1^o) for the middle one and (2%, 2^o) for the bottom plot. The horizontal red line corresponds to 1 Watts/m, a suggested limit for hands-on maintenance. The numbered arrows on the top indicate the beginning of a new section according to table 2.

beam loss analysis showed that the actual design produce very limited beam loss in both fraction and peak power loss for the typical values of both misalignment and RF errors.

REFERENCES

[1] G.W. Foster and J.A. MacLachlan, Proceedings. of LINAC-2002 Conference, p.826.

[2] V.N. Aseev et al, Proceedings of PAC-05 Conference, Knoxville, Tennessee, May 16-20, 2005.

[3] P.N. Ostroumov, V. N. Aseev, and A.A. Kolomiets, J. of Instr., JINST 1, P04002, 2006

[4] K.W. Shepard et al, Proceedings of PAC-05 Conference, Knoxville, Tennessee, May 16-20, 2005.

[5] TESLA Technical Design Report, DESY 2001-11 at http://tesla.desy.de/new_pages/TDR_CD/PartII/accel.html

[6] P.N. Ostroumov et al, Proceedings of HB-2006 Workshop, Tsukuba, Japan, May 29-June 2, 2006.

[7] P.N. Ostroumov and K.W. Shepard, Phys. Rev. ST. Accel. Beams 4, 110101 (2001)

[8] P.N. Ostroumov, J.A. Nolen and B. Mustapha, Nucl. Instr. and Meth. A 558 (2006) 25

[9] P.N. Ostroumov, V. N. Aseev, and B. Mustapha. Phys. Rev. ST. Accel. Beams 7, 090101 (2004).

[10] B. Mustapha and P.N. Ostroumov, Phys. Rev. ST. Accel. Beams 8, 090101 (2005).

[11] Jazz web site: http://www.lcrc.anl.gov